Shilnikov sense chaos in a simple three-dimensional system*

Wang Wei(王 炜)[a)], Zhang Qi-Chang(张琪昌)[a)†], and Tian Rui-Lan(田瑞兰)[b)]

[a)] *Department of Mechanics, School of Mechanical Engineering, Tianjin University, Tianjin* 300072, *China*
[b)] *Centre for Nonlinear Dynamics Research, Shijiazhuang Railway Institute, Shijiazhuang* 050043, *China*

(Received 2 January 2009; revised manuscript received 21 September 2009)

The Shilnikov sense Smale horseshoe chaos in a simple 3D nonlinear system is studied. The proportional integral derivative (PID) controller is improved by introducing the quadratic and cubic nonlinearities into the governing equations. For the discussion of chaos, the bifurcate parameter value is selected in a reasonable regime at the requirement of the Shilnikov theorem. The analytic expression of the Shilnikov type homoclinic orbit is accomplished. It depends on the series form of the manifolds surrounding the saddle-focus equilibrium. Then the methodology is extended to research the dynamical behaviours of the simplified solar-wind-driven-magnetosphere-ionosphere system. As is illustrated, the Lyapunov characteristic exponent spectra of the two systems indicate the existence of chaotic attractor under some specific parameter conditions.

Keywords: chaos, Shilnikov theorem, homoclinic orbit, manifold
PACC: 0547, 4660D, 0340

1. Introduction

In recent years, there has been a great deal of interest in understanding the dynamics and bifurcations in problems governed by three-dimensional (3D) autonomous differential systems. These problems include sequences of periodic doubling, existence of the strange attractor, and bifurcations creating the horseshoe chaos. The most important tool for analysing the chaotic motion of a 3D nonlinear dynamical system is the well-known Shilnikov theorem. On the basis of the work by Shilnikov, the chaotic behaviour is exhibited in the neighbourhoods of parameter space where certain homoclinic orbits appear, surrounding the saddle-focus equilibrium point.[1] Thus, the eigenvalues of the Jacobian characteristic polynomial and the existence of homoclinic orbit have been frequently discussed in academic researches. Since the discovery of the famous Lorenz chaotic system, researchers think much of seeking some kind of canonical forms of all possible continuous time quadratic autonomous chaotic systems in three dimensions, in particular, simple chaotic systems with quadratic nonlinearity such as the Lorenz and Rössler systems.[2−6] Zhang *et al.*[2] discussed the properties of mechanically and electrically coupled nonlinear dynamical systems, based on the Shilnikov criterion, and presented a rigorous proof of the existence of horseshoe chaos. Zhou *et al.*[3] constructed a new chaotic system of quadratic polynomial ordinary differential equations of three dimensions with a single equilibrium point, where numerical simulation demonstrated the route to chaos through flip bifurcation. Li *et al.*[4] presented a mathematically rigorous proof for the existence of the chaos in a modified Lorenz system using the theory of Shilnikov bifurcations and homoclinic and heteroclinic orbits. Genesio *et al.*[5] studied the well-known Rössler system and pointed out the main complex dynamics which can be exhibited, and also gave indications to predict possible homoclinic orbits with the unifying approach by a harmonic balance technique. The existence of Shilnikov sense orbit was predicted in coupled Duffing equation by using Melnikov method and geometrical singular perturbation theory by Xu and Jing.[6] They declared there would be Smale horseshoe in the system as well as chaotic motion.

As compared with the mathematic proof for the existence of the chaotic attractor and homoclinic orbit in the system, the orbits themselves have not received enough attention except the Lorenz-type canonical form. Mikhlin[7] used the quasi-Padé approximation for the construction of homoclinic orbits of nonlinear Schrödinger equation and Lorenz system. Vakakis and Azeez[8] expressed the solution in power series as $t \to \pm 0$ and introduced global approximants to match the local solutions by means of Padé-like procedure.

*Project supported by the National Natural Science Foundation of China (Grant No. 10872141).
†Corresponding author. E-mail: qzhang@tju.edu.cn
© 2010 Chinese Physical Society and IOP Publishing Ltd

Based on the characteristics of a type of n-dimensional quadratic system, Li and Zhu[9] constructed the s-dimensional ($s \leq n$) series expression of the stable and unstable manifolds, which formed homoclinic orbit near the hyperbolic singular point of the Lorenz system. So there still need more attention to be paid especially to the analytically approximate Shilnikov-type homoclinic structure for the atypical systems as presented in this article.

In this work, we first study the Shilnikov sense Smale horseshoe chaos in a modified PID controller. The 3D system is distinguished from the Lorenz-type canonical form with quadratic and cubic nonlinearity. The parameter value of chaotic motion is limited to the requirement of the Shilnikov theorem. In view of the homoclinic orbit, the rigorous proof for its existence is pursued as mentioned before.[2−6] We also adjust series expressions of the stable and unstable manifolds of the saddle-focus equilibrium to form the Shilnikov-type homoclinic loop. The whole procedure of discussion is further extended to the research of the dynamical behaviours of the reduced solar-wind-driven-magnetosphere-ionosphere system. As is illustrated, the Lyapunov characteristic exponent spectra of the two systems provide a convictive proof of the existence of chaotic attractor under some specific parameter conditions.

2. Shilnikov theorem

Shilnikov proved that a saddle-focus homoclinic orbit under certain conditions has in its neighbourhood a countable set of periodic trajectories which can lead to the formation of chaotic attractor. For chaos to occur within a 3D phase space, it requires the system to satisfy

$$\frac{\mathrm{d}x}{\mathrm{d}t} = f(x), \quad t \in \mathbb{R}, \ \boldsymbol{x} \in \mathbb{R}^3, \tag{1}$$

where the vector field $f : \mathbb{R}^3 \to \mathbb{R}^3$ is p-times differentiable ($p \geq 1$) with a continuous derivative (so called C^p), and $\mathbb{R}^3$ stands for the real space of dimension three. We call the equilibrium point $\boldsymbol{x}_0 \in \mathbb{R}^3$, a hyperbolic saddle-focus, if the eigenvalues of the 3×3 real matrix $\boldsymbol{A} = Df(\boldsymbol{x}_0)$, the Jacobian derivative of f at $\boldsymbol{x}_0$, are of the form

$$\lambda_1 = r, \ \ \lambda_{2,3} = p \pm \mathrm{i}\, q, \ \ rp < 0, \ \ q \neq 0, \tag{2}$$

where r, p and q are real. Given the background, the Shilnikov theorem will be described as follows:

Shilnikov theorem The 3D autonomous system is given in Eq. (1). Let $\boldsymbol{x}_0$ be an equilibrium point of Eq. (1), whose characteristic eigenvalues satisfy $r < 0, p > 0$, $|r| > p$, and there exists a homoclinic orbit Γ at $\boldsymbol{x}_0$. The original system exhibits horseshoe chaos.[1,10]

3. Eigenvalues analysis of the PID controller

We consider a 3D system

$$\begin{aligned} \dot{x} &= y + \rho x z, \\ \dot{y} &= z + \nu x y, \\ \dot{z} &= -\alpha x - \beta y - \gamma z + \delta x^2 + \kappa x^3, \end{aligned} \tag{3}$$

which is formally evolved from the 3D PID controller

$$\begin{aligned} \dot{x} &= y, \\ \dot{y} &= z, \\ \dot{z} &= -bx - ay - \kappa z + \delta x^3 \end{aligned} \tag{4}$$

with the primary target of promoting or eliminating chaos.[11] Equation (3) has equilibrium points

$$\boldsymbol{x}_0(0,0,0), \quad \boldsymbol{x}_1\Big(-\frac{\delta + \sqrt{\delta^2 + 4\alpha\kappa}}{2\kappa}, 0, 0\Big), \quad \boldsymbol{x}_2\Big(\frac{-\delta + \sqrt{\delta^2 + 4\alpha\kappa}}{2\kappa}, 0, 0\Big),$$

$$\boldsymbol{x}_3\bigg(-\frac{1}{\sqrt{\nu}\sqrt{\rho}}, \frac{-\kappa + \delta\sqrt{\nu}\sqrt{\rho} + \alpha\nu\rho}{\gamma\nu^2\rho + \beta\nu^{3/2}\rho^{3/2}}, \frac{-\kappa + \delta\sqrt{\nu}\sqrt{\rho} + \alpha\nu\rho}{\gamma\nu^{3/2}\rho^{3/2} + \beta\nu\rho^2}\bigg),$$

$$\boldsymbol{x}_4\bigg(\frac{1}{\sqrt{\nu}\sqrt{\rho}}, -\frac{\kappa + \delta\sqrt{\nu}\sqrt{\rho} - \alpha\nu\rho}{\gamma\nu^2\rho - \beta\nu^{3/2}\rho^{3/2}}, \frac{\kappa + \delta\sqrt{\nu}\sqrt{\rho} - \alpha\nu\rho}{\gamma\nu^{3/2}\rho^{3/2} - \beta\nu\rho^2}\bigg).$$

Here we only discuss the origin $\boldsymbol{x}_0$, and using the Jacobian matrix

$$\boldsymbol{A} = \begin{bmatrix} 0 & 1 & 0 \\ 0 & 0 & 1 \\ -\alpha & -\beta & -\gamma \end{bmatrix}, \tag{5}$$

we have the characteristic polynomial

$$\lambda^3 + \gamma\lambda^2 + \beta\lambda + \alpha = 0. \tag{6}$$

Supposing $\lambda = \mu - \dfrac{\gamma}{3}$, we can have Eq. (5) in the following form

$$\mu^3 + m\mu + n = 0, \tag{7}$$

where

$$m = \beta - \frac{\gamma^2}{3}, \quad n = \alpha - \frac{\beta\gamma}{3} + \frac{2\gamma^3}{27}.$$

Then the Cardano formula ensures the roots of Eq. (7) to meet the requirement of Shilnikov theorem. It yields

$$\begin{aligned} &\Delta = \left(\frac{m}{2}\right)^3 + \left(\frac{n}{3}\right)^2 > 0, \\ &\sqrt[3]{-\frac{n}{2} + \sqrt{\Delta}} - \sqrt[3]{\frac{n}{2} + \sqrt{\Delta}} < \min\left(-\frac{2\gamma}{3}, \frac{\gamma}{3}\right). \end{aligned} \tag{8}$$

That means Eq. (6) has one real root and a conjugate pair of complex roots, while the real root is negative and the real part of the complex conjugate roots is positive. So the equilibrium point $\boldsymbol{x}_0$ is of saddle-focus type and the eigenvalues meet the condition $r < 0, p > 0$, $|r| > p$ as it is required.

Thus, there is only demand to prove that Eq. (3) has a homoclinic orbit connecting the point $\boldsymbol{x}_0$ to confirm the existence of chaotic attractor.

4. Existence of the homoclinic orbit

For discussing the homoclinic orbit of $\boldsymbol{x}_0$, it can be supposed that the series form, is like

$$\begin{aligned} x(t) &= \sum_{k=1}^{+\infty} a_k \mathrm{e}^{k\lambda_1 t}, \\ y(t) &= \sum_{k=1}^{+\infty} b_k \mathrm{e}^{k\lambda_1 t}, \\ z(t) &= \sum_{k=1}^{+\infty} c_k \mathrm{e}^{k\lambda_1 t}, \quad t > 0, \end{aligned} \tag{9}$$

where $a_0 = b_0 = c_0 = 0$, and λ_1 is the negative eigenvalue.

For $k = 1$, substituting Eq. (9) into Eq. (3) and matching the coefficients of $\mathrm{e}^{k\lambda_1 t}$ on both sides of the resulting equation, give

$$(\lambda_1 \boldsymbol{I} - \boldsymbol{A}) \begin{bmatrix} a_1 \\ b_1 \\ c_1 \end{bmatrix} = 0, \tag{10}$$

where $\boldsymbol{A}$ is the Jacobian matrix evaluated at the point $\boldsymbol{x}_0$. We know $\det(\lambda_1 \boldsymbol{I} - \boldsymbol{A}) = 0$, so $(a_1, b_1, c_1) \neq 0$ and can be expressed with an arbitrary parameter ξ.

In the case of $k > 1$, we have $\det(k\lambda_1 \boldsymbol{I} - \boldsymbol{A}) \neq 0$, and from the earlier step, we obtain

$$\begin{bmatrix} a_k \\ b_k \\ c_k \end{bmatrix} = (k\lambda_1 \boldsymbol{I} - \boldsymbol{A})^{-1} \begin{bmatrix} \rho \sum\limits_{i+j=1}^{k} a_i c_j \\ \nu \sum\limits_{i+j=1}^{k} a_i b_j \\ \gamma \sum\limits_{i+j=1}^{k} a_i a_j + \kappa \sum\limits_{i+j+m=1}^{k} a_i a_j a_m \end{bmatrix}. \tag{11}$$

This means that the undetermined coefficients $(a_k,\ b_k,\ c_k)$ can be determined uniquely. For the reverse trajectories of $\boldsymbol{x}_0$ at $t < 0$, the original system turns to

$$\begin{aligned} \dot{x} &= -y - \rho xz, \\ \dot{y} &= -z - \nu xy, \\ \dot{z} &= \alpha x + \beta y + \gamma z - \delta x^2 - \kappa x^3, \end{aligned} \tag{12}$$

in terms of the new time transformation $\tau = -t$. Following the similar procedure, homoclinic orbit at equilibrium

point $\boldsymbol{x}_0$ is formally obtained as

$$x(t)=\begin{cases}\sum\limits_{k=1}^{+\infty}a_k\mathrm{e}^{k\lambda_1 t},t\geq 0,\\ \sum\limits_{k=1}^{+\infty}a'_k\mathrm{e}^{-k\lambda_1 t},t<0,\end{cases}\quad y(t)=\begin{cases}\sum\limits_{k=1}^{+\infty}b_k\mathrm{e}^{k\lambda_1 t},t\geq 0,\\ \sum\limits_{k=1}^{+\infty}b'_k\mathrm{e}^{-k\lambda_1 t},t<0,\end{cases}\quad z(t)=\begin{cases}\sum\limits_{k=1}^{+\infty}c_k\mathrm{e}^{k\lambda_1 t},t\geq 0,\\ \sum\limits_{k=1}^{+\infty}c'_k\mathrm{e}^{-k\lambda_1 t},t<0,\end{cases}. \tag{13}$$

where $\sum\limits_{k=1}^{+\infty}a_k=\sum\limits_{k=1}^{+\infty}a'_k$, $\sum\limits_{k=1}^{+\infty}b_k=\sum\limits_{k=1}^{+\infty}b'_k$, $\sum\limits_{k=1}^{+\infty}c_k=\sum\limits_{k=1}^{+\infty}c'_k$.

So, in the 3D space, the horseshoe chaos may be expected to occur in a reasonable regime from the requirement of the Shilnikov theorem.

5. Shilnikov sense chaos of the controller

The system is evaluated for $\alpha=2.1$, $\gamma=0.45$, $\delta=1$, $\kappa=3.3$, $\rho=0.05$, $\nu=0.07$, so chaos is expected to occur in the range of $0.0646801\leq\beta<4.71283$, obtained from Eq. (7). In Fig. 1, the projections of the chaotic attractor on $(x-y)$, $(y-z)$, $(x-z)$ planes at the value of $\beta=2$ are plotted, meanwhile the chaotic time series of trajectory $x(t)$, $y(t)$, and $z(t)$ appear in Fig. 2. Finally the 3D phase portrait of the chaotic attractor is shown in Fig. 3.

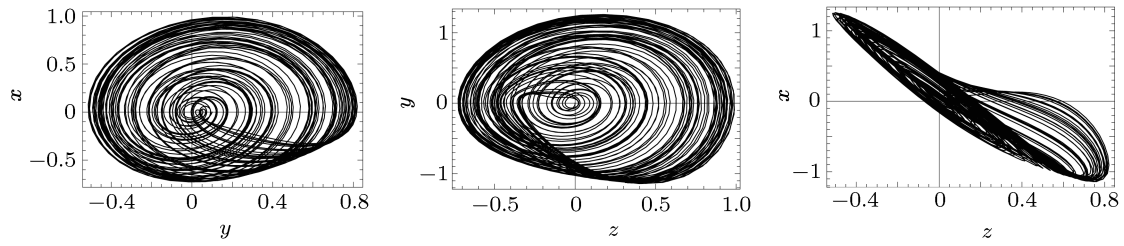


Fig. 1. Projections of the chaotic attractor on $(x-y)$, $(y-z)$, and $(x-z)$ planes.

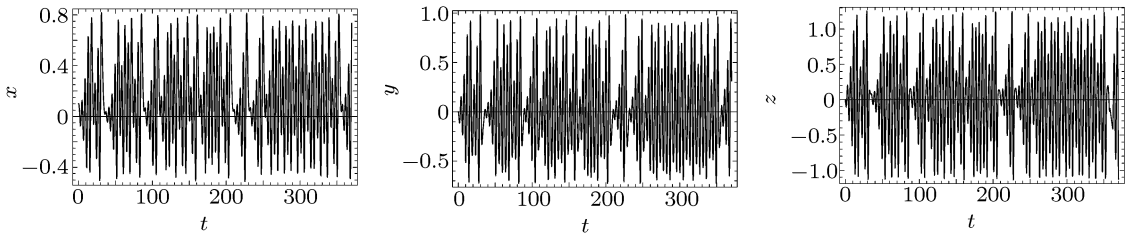


Fig. 2. Chaotic time series of trajectory $x(t)$, $y(t)$, and $z(t)$.

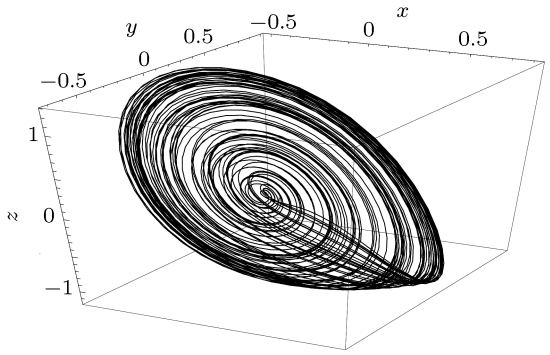


Fig. 3. The 3D phase portrait for chaos.

Next, we use the Lyapunov characteristic exponent to analyse the presence of the chaotic attractor. The exponent allows the generalisation of the linear stability analysis from perturbations of steady state solutions to those of time-dependent solutions, and also provides a meaningful way to characterise the asymptotic behaviour of nonlinear dynamics. For time series produced by dynamical systems, the presence of a positive characteristic exponent indicates chaos[12,13] So with the help of computer algebra Mathematica the exponent spectrum of Eq. (3) is illustrated in Fig. 4. The positive characteristic exponent ($l_1=0.114238$) provides a powerful witness to the analytical estima-

tion.

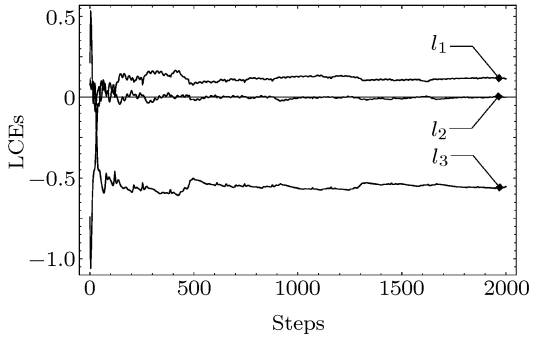


Fig. 4. Lyapunov spectrum for the PID controller.

6. Analytical expression of the homoclinic orbit

The existence of homoclinic orbit has been theoretically verified and the chaotic attractor is also numerically obtained at the exact parameter values for the orbit. But what we want to know is not the form but the analytical expression of the orbit. That is far beyond the reach of 1D manifold with the eigenvalue λ_1; and the 2D structure, as shown in the Lorenz system,[9] requires to be concerned with as well. So we begin with the analytical expressions of the 1D manifold in Eq. (3)

$$x(t)=\sum_{m=0}^{k}a_m\mathrm{e}^{m\lambda_1 t},\quad y(t)=\sum_{m=0}^{k}b_m\mathrm{e}^{m\lambda_1 t},$$
$$z(t)=\sum_{m=0}^{k}c_m\mathrm{e}^{m\lambda_1 t}, \tag{14}$$

where a_m, b_m and c_m are the undetermined coefficients as before. Differentiate Eq. (14) with respect to time t and substitute into Eq. (3) simultaneously, and then balance the same order terms of $\mathrm{e}^{m\lambda_1 t}$ on both sides of the resulting equation. This yields the results

$$m\lambda_1 a_m=b_m+\rho\sum_{j=0}^{m}a_jc_{m-j},\quad m\lambda_1 b_m=c_m+\nu\sum_{j=0}^{m}a_jb_{m-j},$$
$$m\lambda_1 c_m=-\alpha a_m-\beta b_m-\gamma c_m+\delta\sum_{j=0}^{m}a_ja_{m-j}+\kappa\sum_{j=0}^{m}\sum_{h=0}^{m-j}a_ja_ha_{m-j-h}, \tag{15}$$

where the subscript $j+k>0$, and $a_0=b_0=c_0=0$. We obtain the undetermined coefficients step by step in the range of $m\in[1,k]$. Because $(a_m,b_m,c_m)\neq(0,0,0)$, when $\det(\lambda_1\boldsymbol{I}-\boldsymbol{A})=0$, $(a_1,\ b_1,\ c_1)$ is produced in terms of the eigenvectors $v_{1,j}$ of eigenvalue λ_1,

$$a_1=\mu_1v_{1,1},\quad b_1=\mu_1v_{1,2},\quad c_1=\mu_1v_{1,3},\quad \mu_1\in[-\mu_{1m},\mu_{1m}], \tag{16}$$

where μ_{1m} is the maximum constant to keep series expression convergent. This means that in the range of $-\mu_{1m}\leq\mu_1\leq\mu_{1m}$, Eq. (14) is a convergent series, while divergent out of the range.[9]

As for the order of $m=2,\cdots,k$, from Eq. (15), it yields the explicit iterative formulas of the coefficients corresponding to $(a_k,\ b_k,\ c_k)$,

$$\begin{aligned}a_k=&[(k^2\lambda_1^2+\beta+k\lambda_1\gamma)\rho\sum_{j=1}^{k-1}a_jc_{k-1-j}+(k\lambda_1+\gamma)\nu\sum_{j=1}^{k-1}a_jb_{k-1-j}+\delta\sum_{j=1}^{k-1}a_ja_{k-1-j}\\&+\kappa\sum_{j=1}^{k-1}\sum_{h=1}^{k-1-j}a_ja_ha_{k-1-j-h}]/\{\alpha+k\lambda_1[\beta+k\lambda_1(\gamma+k\lambda_1)]\},\\b_k=&\Big\{-\alpha\rho\sum_{j=1}^{k-1}a_jc_{k-1-j}+k\lambda_1[\delta\sum_{j=1}^{k-1}a_ja_{k-1-j}+\kappa\sum_{j=1}^{k-1}\sum_{h=1}^{k-1-j}a_ja_ha_{k-1-j-h}\\&+\nu\sum_{j=1}^{k-1}a_jb_{k-1-j}\,(\gamma+k\lambda_1)]\Big\}/\{\alpha+k\lambda_1[\beta+k\lambda_1(\gamma+k\lambda_1)]\},\\c_k=&\Big\{-\nu\sum_{j=1}^{k-1}a_jb_{k-1-j}[\alpha+k\beta\lambda_1]+k\lambda_1[-\alpha\rho\sum_{j=1}^{k-1}a_jc_{k-1-j}+k(\delta\sum_{j=1}^{k-1}a_ja_{k-1-j}\\&+\kappa\sum_{j=1}^{k-1}\sum_{h=1}^{k-1-j}a_ja_ha_{k-1-j-h})\lambda_1]\Big\}/\{\alpha+k\lambda_1[\beta+k\lambda_1(\gamma+k\lambda_1)]\}.\end{aligned} \tag{17}$$

The 2D manifold expressions of $\lambda_{2,3}$ in Eq. (3) are

$$x(t)=\sum_{m=0}^{k}\sum_{n=0}^{k-m}a_{m,n}\mathrm{e}^{(m\lambda_2 t+n\lambda_3 t)},\quad y(t)=\sum_{m=0}^{k}\sum_{n=0}^{k-m}b_{m,n}\mathrm{e}^{(m\lambda_2 t+n\lambda_3 t)},$$
$$z(t)=\sum_{m=0}^{k}\sum_{n=0}^{k-m}c_{m,n}\mathrm{e}^{(m\lambda_2 t+n\lambda_3 t)}, \tag{18}$$

where $a_{m,n},\ b_{m,n}$ and $c_{m,n}$ are the undetermined coefficients. Differentiate Eq. (17) with respect to time t and substitute into Eq. (3) simultaneously, and then balance the same order terms of $\mathrm{e}^{(m\lambda_2 t+n\lambda_3 t)}$ on both sides of the resulting equation. The results become a little complicated and are required to be treated separately, including $m>0, n=0$; $m=0, n>0$; and $m>0, n>0$. So,

$$m\lambda_2 a_{m,0}=b_{m,0}+\rho\sum_{m_1=0}^{m}a_{m_1,0}c_{m-m_1,0},\quad m\lambda_2 b_{m,0}=c_{m,0}+\nu\sum_{m_1=0}^{m}a_{m_1,0}b_{m-m_1,0},$$
$$m\lambda_2 c_{m,0}=-\alpha a_{m,0}-\beta b_{m,0}-\gamma c_{m,0}+\delta\sum_{m_1=0}^{m}a_{m_1,0}a_{m-m_1,0}$$
$$+\kappa\sum_{m_1=0}^{m}\sum_{m_2=0}^{m-m_1}a_{m_1,0}a_{m_2,0}a_{m-m_1-m_2,0};\quad (\text{for } m>0,\ n=0) \tag{19}$$

$$n\lambda_3 a_{0,n}=b_{0,n}+\rho\sum_{n_1=0}^{n}a_{0,n_1}c_{0,n-n_1},\quad n\lambda_3 b_{0,n}=c_{0,n}+\nu\sum_{n_1=0}^{n}a_{0,n_1}b_{0,n-n_1},$$
$$n\lambda_3 c_{0,n}=-\alpha a_{0,n}-\beta b_{0,n}-\gamma c_{0,n}+\delta\sum_{n_1=0}^{n}a_{0,n_1}a_{0,n-n_1}$$
$$+\kappa\sum_{n_1=0}^{n}\sum_{n_2=0}^{n-n_1}a_{0,n_1}a_{0,n_2}a_{0,n-n_1-n_2};\quad (\text{for } m=0,\ n>0) \tag{20}$$

$$(m\lambda_2+n\lambda_3)a_{m,n}=b_{m,n}+\rho\sum_{m_1=0}^{m}\sum_{n_1=0}^{n}a_{m_1,n_1}c_{m-m_1,n-n_1},$$
$$(m\lambda_2+n\lambda_3)b_{m,n}=c_{m,n}+\nu\sum_{m_1=0}^{m}\sum_{n_1=0}^{n}a_{m_1,n_1}b_{m-m_1,n-n_1},$$
$$(m\lambda_2+n\lambda_3)c_{m,n}=-\alpha a_{m,n}-\beta b_{m,n}-\gamma c_{m,n}+\delta\sum_{m_1=0}^{m}\sum_{n_1=0}^{n}a_{m_1,n_1}a_{m-m_1,n-n_1}$$
$$+\kappa\sum_{m_1=0}^{m}\sum_{n_1=0}^{n}\sum_{m_2=0}^{m-m_1}\sum_{n_2=0}^{n-n_1}a_{m_1,n_1}a_{m_2,n_2}a_{m-m_1-m_2,n-n_1-n_2}.\quad (\text{for } m>0,\ n>0) \tag{21}$$

In Eqs. (19)–(21), $m_1+m_2+n_1+n_2>0$ is required, and the first-order terms $(a_{0,0}, b_{0,0}, c_{0,0})$ amount to zero because of the homoclinic orbit passing the equilibrium point $\boldsymbol{x}_0$. So the undetermined coefficients $a_{m,n},\ b_{m,n}$ and $c_{m,n}$ in Eq. (18) can be determined orderly, as $m+n\in[1,2,\ldots,k]$. Employing the eigenvectors $v_{i,j}$ of the complex eigenvalues $\lambda_{2,3}$ for the first-order $m+n=1$ yields

$$a_{1,0}=\mu_2 v_{2,1},\quad b_{1,0}=\mu_2 v_{2,2},\quad c_{1,0}=\mu_2 v_{2,3},\quad a_{0,1}=\mu_3 v_{3,1},\quad b_{0,1}=\mu_3 v_{3,2},\quad c_{0,1}=\mu_3 v_{3,3}, \tag{22}$$

where $\mu_i\in[-\mu_{im},\mu_{im}]$, $i=2,3$, and μ_{im} is the maximum constant to keep series expression (18) convergent.[9]

As for $m+n=k$, we proclaim the results in terms of $m=k,\ n=0$; $m=0,\ n=k$; and $m=j,\ n=k-j$. From Eqs. (19)–(21), we have, for $m=k,\ n=0$

$$a_{k,0}=\frac{\delta P_{k,0,a^2}+\kappa P_{k,0,a^3}+\nu P_{k,0,ab}(\gamma+k\lambda_2)+\rho P_{k,0,ac}[\beta+k\lambda_2(\gamma+k\lambda_2)]}{\alpha+k\lambda_2[\beta+k\lambda_2(\gamma+k\lambda_2)]},$$
$$b_{k,0}=\frac{-\alpha\rho P_{k,0,ac}+k\lambda_2[\delta P_{k,0,a^2}+\kappa P_{k,0,a^3}+\nu P_{k,0,ab}(\gamma+k\lambda_2)]}{\alpha+k\lambda_2[\beta+k\lambda_2(\gamma+k\lambda_2)]},$$

$$c_{k,0}=\frac{-\nu P_{k,0,ab}(\alpha+k\beta\lambda_2)+k\lambda_2[-\alpha\rho P_{k,0,ac}+k(\delta P_{k,0,a^2}+\kappa P_{k,0,a^3})\lambda_2]}{\alpha+k\lambda_2[\beta+k\lambda_2(\gamma+k\lambda_2)]}, \tag{23}$$

where

$$P_{k,0,ab}=\sum_{j_1=1}^{k-1}a_{j_1,0}b_{k-1-j_1,0}, P_{k,0,ac}=\sum_{j_1=1}^{k-1}a_{j_1,0}c_{k-1-j_1,0}, P_{k,0,a^2}=\sum_{j_1=1}^{k-1}a_{j_1,0}a_{k-1-j_1,0},$$
$$P_{k,0,a^3}=\sum_{j_1=1}^{k-1}\sum_{j_2=1}^{k-1-j_1}a_{j_1,0}a_{j_2,0}a_{k-1-j_1-j_2,0};$$

for $m=0,\ n=k$, we have

$$\begin{aligned}
a_{0,k}&=\frac{\delta P_{0,k,a^2}+\kappa P_{0,k,a^3}+\nu P_{0,k,ab}(\gamma+k\lambda_3)+\rho P_{0,k,ac}[\beta+k\lambda_3(\gamma+k\lambda_3)]}{\alpha+2\lambda_2[\beta+2\lambda_2(\gamma+2\lambda_2)]},\\
b_{0,k}&=\frac{-\alpha\rho P_{0,k,ac}+k\lambda_3[\delta P_{0,k,a^2}+\kappa P_{0,k,a^3}+\nu P_{0,k,ab}(\gamma+k\lambda_3)]}{\alpha+2\lambda_2[\beta+2\lambda_2(\gamma+2\lambda_2)]},\\
c_{0,k}&=\frac{-\nu P_{0,k,ab}(\alpha+k\beta\lambda_3)+k\lambda_3[-\alpha\rho P_{0,k,ac}+k(\delta P_{0,k,a^2}+\kappa P_{0,k,a^3})\lambda_3]}{\alpha+2\lambda_2[\beta+2\lambda_2(\gamma+2\lambda_2)]},
\end{aligned} \tag{24}$$

where

$$P_{0,k,ab}=\sum_{j_1=1}^{k-1}a_{0,j_1}b_{0,k-1-j_1}, P_{0,k,ac}=\sum_{j_1=1}^{k-1}a_{0,j_1}c_{0,k-1-j_1}, P_{0,k,a^2}=\sum_{j_1=1}^{k-1}a_{0,j_1}a_{0,k-1-j_1},$$
$$P_{0,k,a^3}=\sum_{j_1=1}^{k-1}\sum_{j_2=1}^{k-1-j_1}a_{0,j_1}a_{0,j_2}a_{0,k-1-j_1-j_2};$$

for $m=j,\ n=k-j$

$$\begin{aligned}
a_{j,k-j}=&\{\delta P_{j,k-j,a^2}+\kappa P_{j,k-j,a^3}+\nu P_{j,k-j,ab}[\gamma+j\lambda_2+(k-j)\lambda_3]\\
&+\rho P_{j,k-j,ac}\{\beta+[j\lambda_2+(k-j)\lambda_3][\gamma+j\lambda_2+(k-j)\lambda_3]\}\}\\
&/\{\alpha+[j\lambda_2+(k-j)\lambda_3]\{\beta+[j\lambda_2+(-j+k)\lambda_3][\gamma+j\lambda_2+(k-j)\lambda_3]\}\},\\
b_{j,k-j}=&\{-\alpha\rho P_{j,k-j,ac}+[j\lambda_2+(k-j)\lambda_3]\{\delta P_{j,k-j,a^2}+\kappa P_{j,k-j,a^3}\\
&+\nu P_{j,k-j,ab}[\gamma+j\lambda_2+(k-j)\lambda_3]\}\}\\
&/\{\alpha+[j\lambda_2+(k-j)\lambda_3]\{\beta+[j\lambda_2+(-j+k)\lambda_3][\gamma+j\lambda_2+(k-j)\lambda_3]\}\},\\
c_{j,k-j}=&\{-\nu P_{j,k-j,ab}[\alpha+j\beta\lambda_2+(k-j)\beta\lambda_3]+[j\lambda_2+(k-j)\lambda_3]\{-\alpha\rho P_{j,k-j,ac}\\
&+(\delta P_{j,k-j,a^2}+\kappa P_{j,k-j,a^3})[j\lambda_2+(k-j)\lambda_3]\}\}\\
&/\{\alpha+[j\lambda_2+(k-j)\lambda_3]\{\beta+[j\lambda_2+(-j+k)\lambda_3][\gamma+j\lambda_2+(k-j)\lambda_3]\}\},
\end{aligned} \tag{25}$$

where

$$P_{j,k-j,ab}=\sum_{j_1=1}^{j}\sum_{h=1}^{k-1-j}a_{j_1,h}b_{j-j_1,k-1-j-h},\quad P_{j,k-j,ac}=\sum_{j_1=1}^{j}\sum_{h=1}^{k-1-j}a_{j_1,h}c_{j-j_1,k-1-j-h},$$
$$P_{j,k-j,a^2}=\sum_{j_1=1}^{j}\sum_{h=1}^{k-1-j}a_{j_1,h}a_{j-j_1,k-1-j-h},$$
$$P_{j,k-j,a^3}=\sum_{j_1=1}^{j}\sum_{h_1=1}^{k-1-j_1}\sum_{j_2=1}^{k-1-j_1-h_1}\sum_{h_2=1}^{k-1-j_1-j_2-h_1}a_{j_1,h_1}a_{j_2,h_2}a_{j-j_1-j_2,k-1-j_1-j_2-h_1-h_2}.$$

So the invariant manifolds of the 3D system, Eq. (3), have been analytically determined that leads to the series expression of Shilnikov-type homoclinic orbit at the exact parameter values $\alpha=2.1,\ \beta=2,\ \gamma=0.45,\ \delta=1,\ \kappa=3.3,\ \rho=0.05,\ \nu=0.07$. When $k=5$, the equations are

$$\begin{aligned}
x(t)=&\,0.0000904086\mathrm{e}^{-4.40991t}-0.00209339\mathrm{e}^{-3.52793t}-0.0126624\mathrm{e}^{-2.64595t}\\
&+0.0351572\mathrm{e}^{-1.76396t}+0.285672\mathrm{e}^{-0.881982t},
\end{aligned}$$

$$
\begin{aligned}
y(t) &= 0.0000904086\mathrm{e}^{-4.40991t} - 0.00209339\mathrm{e}^{-3.52793t} - 0.0126624\mathrm{e}^{-2.64595t} \\
&\quad + 0.0351572\mathrm{e}^{-1.76396t} + 0.285672\mathrm{e}^{-0.881982t}, \\
z(t) &= -0.000491568\mathrm{e}^{-4.40991t} + 0.0070662\mathrm{e}^{-3.52793t} + 0.0347461\mathrm{e}^{-2.64595t} \\
&\quad - 0.0555391\mathrm{e}^{-1.76396t} - 0.251957\mathrm{e}^{-0.881982t},
\end{aligned} \tag{26}
$$

for the 1D invariant manifold; and

$$
\begin{aligned}
x(t) &= 0.157993\mathrm{e}^{0.550718t} + 0.107838\mathrm{e}^{1.10144t} + 0.400501\mathrm{e}^{0.826077t}\cos[1.54683t] \\
&\quad + 0.100552\mathrm{e}^{1.3768t}\cos[1.54683t] - 0.00907654\mathrm{e}^{1.10144t}\cos[3.09366t] \\
&\quad - 0.0157308\mathrm{e}^{1.3768t}\cos[4.64049t] - 0.640735\mathrm{e}^{0.826077t}\sin[1.54683t] \\
&\quad + 0.314708\mathrm{e}^{1.3768t}\sin[1.54683t] - 0.00304752\mathrm{e}^{1.10144t}\sin[3.09366t] + 0.00755326\mathrm{e}^{1.3768t}\sin[4.64049t], \\
y(t) &= 0.0666371\mathrm{e}^{0.550718t} + 0.0670911\mathrm{e}^{1.10144t} - 0.649093\mathrm{e}^{0.826077t}\cos[1.54683t] \\
&\quad + 0.647801\mathrm{e}^{1.3768t}\cos[1.54683t] - 0.072346\mathrm{e}^{1.10144t}\cos[3.09366t] \\
&\quad + 0.0071306\mathrm{e}^{1.3768t}\cos[4.64049t] - 1.14397\mathrm{e}^{0.826077t}\sin[1.54683t] \\
&\quad + 0.281189\mathrm{e}^{1.3768t}\sin[1.54683t] + 0.00712958\mathrm{e}^{1.10144t}\sin[3.09366t] + 0.0884059\mathrm{e}^{1.3768t}\sin[4.64049t], \\
z(t) &= 0.0690365\mathrm{e}^{0.550718t} + 0.0372434\mathrm{e}^{1.10144t} - 2.31284\mathrm{e}^{0.826077t}\cos[1.54683t] \\
&\quad + 1.32849\mathrm{e}^{1.3768t}\cos[1.54683t] - 0.0916256\mathrm{e}^{1.10144t}\cos[3.09366t] \\
&\quad + 0.418036\mathrm{e}^{1.3768t}\cos[4.64049t] + 0.0600869\mathrm{e}^{0.826077t}\sin[1.54683t] \\
&\quad - 0.597752\mathrm{e}^{1.3768t}\sin[1.54683t] + 0.209892\mathrm{e}^{1.10144t}\sin[3.09366t] \\
&\quad + 0.0869272\mathrm{e}^{1.3768t}\sin[4.64049t],
\end{aligned} \tag{27}
$$

for the 2D invariant manifold. These invariant manifolds finally form the Shilnikov-type homoclinic orbit as shown in Fig. 5.

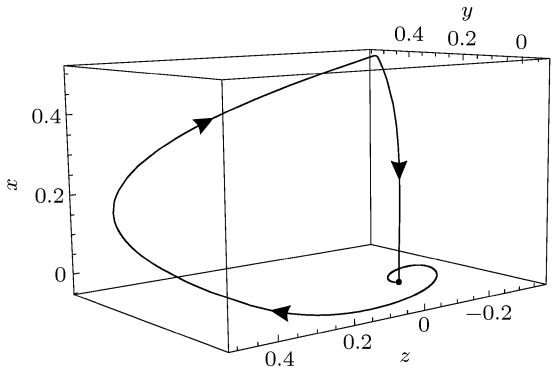


Fig. 5. Shilnikov-type homoclinic orbit of the PID controller.

7. Homoclinic orbit of the simplified WINDMI model

The solar-wind-driven magnetosphere-ionosphere is a complex driven-damped dynamical system. The system exhibits a variety of dynamical states that include low-level steady plasma convection, episodic (quasi-periodic) releases of geotail stored plasma energy into the ionosphere, known widely as substorms, and states of continuous strong unloading provisionally identified as magnetic storms. The model used for the magnetosphere is the WINDMI model, a set of six first-order ordinary differential equations, and well accepted mathematical-physics model for driven-damped magnetosphere-ionosphere system.[14] In Ref. [15], Horton *et al.* considered a reduced form of the WINDMI model. They researched the dynamical features of the following simplified system

$$
\begin{aligned}
&\dot{x} = -y, \quad \dot{y} = c_1 x - b_3 y - z, \\
&\dot{z} = -c_2 - c_3 \tanh x,
\end{aligned} \tag{28}
$$

and analysed the bifurcation property and the nature of the attractor. It can be seen that the essential features of the WINDMI model are basically preserved. That may help to have a better understanding to the importance of assembling large substorm databases with a large range of event sizes.[16] In this article, we want to portrait the chaotic motion of the simplified model and detect the Shilnikov-type homoclinic orbit analytically by using the approach in the foregoing parts.

We evaluate Eq. (28) for the parameter values $c_1 = 1.45$, $c_2 = 28$, $c_3 = 30$, and regard b_3 as the bifurcate governing parameter. So chaos is expected to occur in the range of $b_3 \in (0, 2.08567]$, which is

obtained from Eq. (8). In Fig. 6, the 3D phase portrait refers to the chaotic attractor which is portrayed

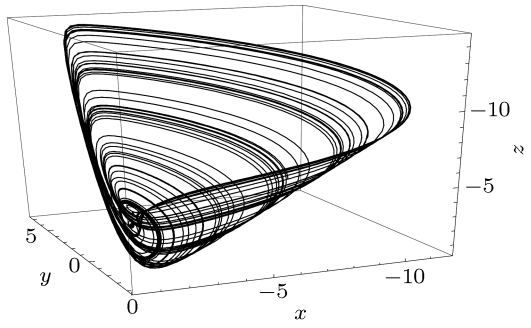


Fig. 6. The 3D phase portrait for to chaos.

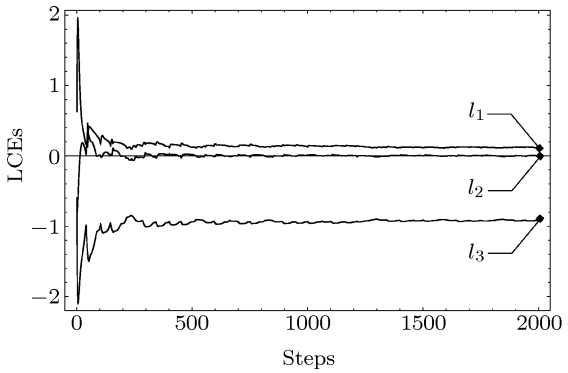


Fig. 7. Lyapunov spectrum for the model.

at the value of $b_3 = 0.8$. We also use the Lyapunov characteristic exponent spectrum of Eq. (29) to illustrate the existence of the Smale horseshoe in Fig. 7. The positive characteristic exponent ($l_1 = 0.11341$) provides a powerful witness to analytical estimation

Then we compute the stable and unstable manifolds of the saddle-focus equilibrium point to construct the Shilnikov-type homoclinic orbit in an analytic style. The reduced system, Eq. (28), has a single equilibrium point

$$(x^*, y^*, z^*) = \left(-\text{arctanh}\left(\frac{c_2}{c_3}\right), 0, -c_1\text{arctanh}\left(\frac{c_2}{c_3}\right)\right). \tag{29}$$

By a simple linear transformation $X = x - x^*$, $Y = y - y^*$, $Z = z - z^*$, we change the coordinates to bring the point $(x^*,\ y^*,\ z^*)$ to the origin, so we obtain

$$\begin{aligned}
\dot{X} &= -Y,\\
\dot{Y} &= c_1 X - b_3 Y - Z,\\
\dot{Z} &= -c_2 - c_3\tanh\left(X - \text{arctanh}\left(\frac{c_2}{c_3}\right)\right).
\end{aligned} \tag{30}$$

Following the methodology of invariant manifolds, the series expressions of homoclinic loop of the reduced system are determined for the 1D and 2D invariant manifolds in Eqs. (31) and (32) at the values of $c_1 = 1.45,\ c_2 = 28,\ c_3 = 30,\ b_3 = 0.8$, when $k = 5$

$$\begin{aligned}
X(t) = {} & -7.20317\times10^{-13}\mathrm{e}^{-7.5993t} + 4.57088\times10^{-10}\mathrm{e}^{-6.07944t} - 2.53709\times10^{-7}\mathrm{e}^{-4.55958t}\\
& + 0.000111184\mathrm{e}^{-3.03972t} - 0.0255781\mathrm{e}^{-1.51986t},\\
Y(t) = {} & -5.4739\times10^{-12}\mathrm{e}^{-7.5993t} + 2.77884\times10^{-9}\mathrm{e}^{-6.07944t} - 1.15681\times10^{-6}\mathrm{e}^{-4.55958t}\\
& + 0.000337968\mathrm{e}^{-3.03972t} - 0.0388751\mathrm{e}^{-1.51986t},\\
Z(t) = {} & -3.82632\times10^{-11}\mathrm{e}^{-7.5993t} + 1.53335\times10^{-8}\mathrm{e}^{-6.07944t} - 4.71698\times10^{-6}\mathrm{e}^{-4.55958t}\\
& + 0.000918172\mathrm{e}^{-3.03972t} - 0.065073\mathrm{e}^{-1.51986t};
\end{aligned} \tag{31}$$

$$\begin{aligned}
X(t) = {} & -0.0464868\mathrm{e}^{0.719862t} - 0.000208301\mathrm{e}^{1.43972t} - 0.0151646\mathrm{e}^{1.07979t}\cos[1.55388t]\\
& + 0.000108782\mathrm{e}^{1.79966t}\cos[1.55388t] + 0.000418883\mathrm{e}^{1.43972t}\cos[3.10776t]\\
& + 7.60283\times10^{-8}\mathrm{e}^{1.79966t}\cos[4.66164t] - 0.00777787\mathrm{e}^{1.07979t}\sin[1.55388t]\\
& - 0.000276183\mathrm{e}^{1.79966t}\sin[1.55388t] - 0.000406827\mathrm{e}^{1.43972t}\sin[3.10776t]\\
& + 0.0000104112\mathrm{e}^{1.79966t}\sin[4.66164t],\\
Y(t) = {} & 0.033464\mathrm{e}^{0.719862t} + 0.000299895\mathrm{e}^{1.43972t} + 0.0284605\mathrm{e}^{1.07979t}\cos[1.55388t]\\
& + 0.000233386\mathrm{e}^{1.79966t}\cos[1.55388t] + 0.000661244\mathrm{e}^{1.43972t}\cos[3.10776t]\\
& - 0.00004867\mathrm{e}^{1.79966t}\cos[4.66164t] - 0.0151655\mathrm{e}^{1.07979t}\sin[1.55388t]\\
& + 0.000666067\mathrm{e}^{1.79966t}\sin[1.55388t] + 0.00188751\mathrm{e}^{1.43972t}\sin[3.10776t]\\
& - 0.0000183821\mathrm{e}^{1.79966t}\sin[4.66164t],
\end{aligned}$$

$$
\begin{aligned}
Z(t) = & -0.118267\mathrm{e}^{0.719862t} - 0.000973718\mathrm{e}^{1.43972t} - 0.0519232\mathrm{e}^{1.07979t}\cos[1.55388t] \\
& - 0.00148398\mathrm{e}^{1.79966t}\cos[1.55388t] - 0.00673954\mathrm{e}^{1.43972t}\cos[3.10776t] \\
& + 0.000212326\mathrm{e}^{1.79966t}\cos[4.66164t] + 0.0614543\mathrm{e}^{1.07979t}\sin[1.55388t] \\
& - 0.00176936\mathrm{e}^{1.79966t}\sin[1.55388t] - 0.0027624\mathrm{e}^{1.43972t}\sin[3.10776t] \\
& - 0.000163999\mathrm{e}^{1.79966t}\sin[4.66164t]. \qquad (32)
\end{aligned}
$$

The orbit of these manifolds formed is illustrated in Fig. 8.

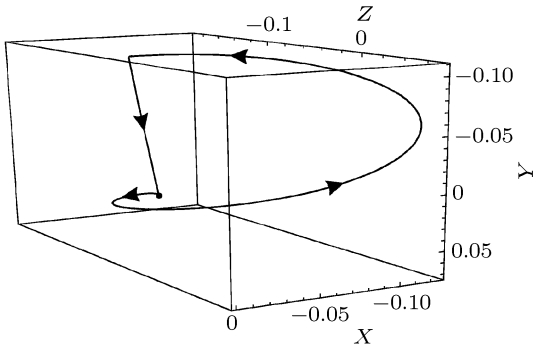


Fig. 8. Shilnikov-type homoclinic orbit of the simplified WINDIMI model.

8. Conclusion

In this article, the strategy of predicting the Shilnikov-sense horseshoe and homoclinic orbit of the new PID controller, as well as the simplified WINDMI model, is presented by using the Shilnikov theorem and the invariant manifolds of the saddle-focus equilibrium point. It provides the quadratic and cubic nonlinearities to the controller systems, which extends the canonical forms of continuous time quadratic autonomous chaotic in 3D system. The Shilnikov type homoclinic orbit is concerned with not only its existence but also the analytical series expression, which distinguishes the present work from the general description of the Shilnikov-sense chaos. We also use the methodology to discuss the complicated dynamical behaviours about a simplified WINDMI system. As is illustrated, the Lyapunov characteristic exponent spectra of the two systems verify the existence of chaotic attractor under some specific parameter conditions.

The strategy presented in this work is sufficiently general, so it would be possible to apply the present method to consider other 3D systems with more complicated nonlinearity, which will be the topic for further research.

References

[1] Shilnikov L P 1970 *Math. USSR-Sbornik* **10** 91
[2] Zhang Q C, Tian R L and Wang W 2008 *Acta Phys. Sin.* **57** 2799 (in Chinese)
[3] Zhou T S, Chen G R and Yang Q G 2004 *Chaos, Solitons and Fractals* **19** 985
[4] Li Z, Chen G R and Halang W A 2004 *Information Sciences* **165** 235
[5] Genesio R, Innocenti G and Gualdani F 2008 *Phys. Lett.* A **372** 1799
[6] Xu P C and Jing Z J 2000 *Chaos, Solitons and Fractals* **11** 853
[7] Mikhlin Y V 2000 *J. Sound Vib.* **230** 971
[8] Vakakis A F and Azeez M F A 1998 *Nonlinear Dynam.* **15** 245
[9] Li Y H and Zhu S M 2006 *Chaos, Solitons and Fractals* **29** 1155
[10] Silva C P 1993 *IEEE Trans. Circuits Syst.* I *Fundam. Theor. Appl.* **40** 675
[11] Cui F S, Chew C H, Xu J X and Cai Y L 1997 *Nonlinear Dynam.* **12** 251
[12] Stenfanski A, Dabrowski A and Kapitaniak T 2005 *Chaos, Solitons and Fractals* **23** 1651
[13] Chen Z M, Djidjdli K and Price W G 2006 *Appl. Math. Comput.* **174** 982
[14] Smith J P, Thiffeault J L and Horton W 2000 *J. Geophys Res.* **105** 12
[15] Horton W, Weigel R S and Sprott J C 2001 *Phys. Plasmas* **8** 2946
[16] Vassiliadis D, Klimas A J, Baker D N and Roberts D A 1996 *J. Geophys. Res.* **101** 19779